Journal of Structural Geology, Vol. 15, No. 7, pp. 849 to 863, 1993
Printed in Great Britain

0191-8141/93 $06.00+0.00

Lateral variations in mylonite zone thickness as influenced by fluid–rock interactions, Linville Falls fault, North Carolina

J. NEWMAN and G. MITRA

Department of Geological Sciences, University of Rochester, Rochester, NY 14627, U.S.A.

(*Received* 10 *February* 1992; *accepted in revised form* 31 *August* 1992)

Abstract—Over a distance of approximately 20 km, along strike, the Linville Falls mylonite varies in thickness from 1 m at Linville Falls to >60 m at Banner Elk. Along strike, pressure, temperature and displacement variations are minimized, allowing this study to focus on the influences of fluid behavior and protolith mineralogy on fault zone development. The protolith at Linville Falls contains mainly K-feldspar, perthite and quartz, while at Banner Elk the protolith contains plagioclase and quartz. At Linville Falls, quartz deformed by dynamic recrystallization, feldspar by intragranular fracturing and alteration to quartz and mica, and mica by sliding along cleavage planes. Modal mineralogies change from the protolith to the mylonite with quartz decreasing from 39 to 19% and feldspar from 59 to 1.5%; muscovite increases from <1 to 80%. Mean grain size of the quartz and feldspar also decreased, from 30 to 20 μm and from 110 to 50 μm, respectively. At Banner Elk, deformation occurred predominantly by dynamic recrystallization within the quartz and by sliding along cleavage planes in mica; no feldspar remains within the mylonite zone. Modal mineralogies change from the protolith to the mylonite with quartz and muscovite increasing from 21 to 50% and from <1 to 44%, respectively. Mean grain size of quartz decreases from 60 to 24 μm.

Mass–balance calculations, based on major- and trace-element geochemistry, indicate approximately 75% volume loss at Linville Falls and 20% at Banner Elk. Fluid–rock ratios estimated from the calculated depletions of Si are an order of magnitude higher at Linville Falls than at Banner Elk. Fluids infiltrated the fault zone over a thicker zone at Banner Elk than at Linville Falls because the plagioclase altered more readily than K-feldspar, creating new pathways for fluids. Fluids migrated preferentially through channels along the fault zone, creating a three-dimensional network of higher fluid flow.

INTRODUCTION

RECENT detailed studies on fault zones have revealed variations in fault zone characteristics (microstructure, mineralogy, grain size, thickness, fluid flow, etc.) both in the transport direction and perpendicular to the transport direction (generally across and along strike, respectively) of major and minor thrust faults (e.g. Schmid 1975, Sibson 1977, Paul & Woodward 1985, Simpson 1985, Wojtal & Mitra 1988). In the transport direction, such variations may have several possible causes.

(i) At any one time, mylonites may be present along one portion of the fault, while cataclasites may dominate along another. Displacement on a fault may carry fault rocks formed at one set of pressure and temperature conditions to different pressure and temperature conditions resulting in overprinting relationships (Gibson & Gray 1985, Simpson 1985, Wojtal & Mitra 1988, Losh 1989).

(ii) With fault propagation, the tip-line of a thrust fault may intersect new lithologies which are then incorporated into the fault zone. Under the same deformation conditions these different lithologies may deform in different manners. Additionally, as displacement along the fault increases, fault zone rocks become progressively more deformed and the microstructure may be sufficiently changed to allow different deformation mechanisms to prevail. For example, a change in grain size due to deformation may result in a change in the dominant deformation mechanism from crystal-plastic or cataclastic to diffusion processes (e.g. Schmid 1975, Mitra 1984).

Perpendicular to the transport direction (along strike) variations in fault zone characteristics occur as well. Along strike, a major thrust fault may intersect different formations, or the lithology of a formation may vary influencing deformation behavior. In addition, fluids play an important role in fault zone behavior, and the amount and composition of fluids infiltrating a fault zone may vary along or across strike resulting in different deformation mechanisms dominating along different segments of the fault.

We studied fault rocks exposed along the strike of the Linville Falls fault zone, North Carolina, where a variation in fault thickness of >60 times occurs over a 20 km distance. Across the strike, the influence of lithology and fluids on fault behavior may be confounded among the many different influences such as pressure, temperature and displacement. Looking along strike, we assume that the present erosion surface approximates a paleolevel section, so that pressure, temperature and displacement were approximately constant. The lithology of the hanging wall rocks are similar, except for the feldspar mineralogy, which changes along strike. Could a change in the type of feldspar influence fault deformation behavior? In this study we describe the deformation along the mylonite zone, determine volume loss and fluid–rock ratios along the mylonite zone using mass–balance calculations based on major and trace

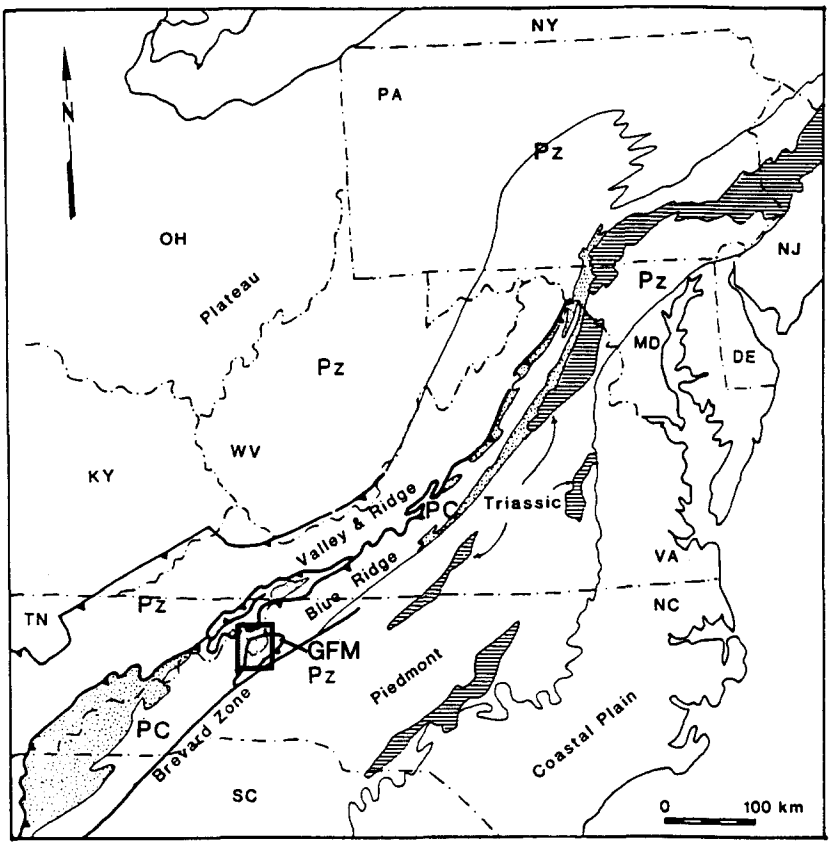

Fig. 1. Location map of the Grandfather Mountain window (GFM) in the southern Blue Ridge, U.S.A. Box shows location of Fig. 2. Lined pattern indicates Triassic rocks; stippled pattern indicates Proterozoic stratified rocks.

element geochemistry, and discuss the influence of lithology, fluids and their interactions on fault deformation behavior.

GEOLOGIC SETTING

The Linville Falls fault lies in the Blue Ridge structural province of the Southern Appalachians in North Carolina (Fig. 1). It is the roof thrust of the Grandfather Mountain tectonic window (Boyer & Elliott 1982) and carries Precambrian granitic basement (in the hanging wall) northwestward over footwall rocks made up of granitic basement, late Proterozoic Grandfather Mountain Formation (arkosic basin sediments) and Cambrian Chilhowee quartzites. A Rb/Sr whole rock isochron on Linville Falls mylonites at Linville Falls yields 302 Ma (Van Camp & Fullagar 1982). We studied the portion of the fault exposed along the western edge of the window, where it dips toward the west-southwest. Crystalline basement in the hanging wall is in fault contact with cover rocks in the footwall which include the Grandfather Mountain Formation arkose to the north and the Chilhowee Group quartzites to the south (Fig. 2). The basement in the hanging wall of the Linville Falls fault on the western edge of the window is Cranberry Gneiss, a metamorphic plutonic complex which makes up a large portion of the Blue Ridge thrust sheet in the Grandfather Mountain area. The Cranberry Gneiss along the northern portion of this fault segment is a quartz diorite gneiss, and in the southern portion it is granite gneiss. The feldspar in the hanging wall rocks of the northern portion is plagioclase, while in the southern portion it is K-feldspar and perthite.

Faults consist of a zone of cataclastic or mylonitic rocks referred to as the fault zone. Between the fault zone and undeformed hanging wall and footwall rocks there is typically a region of protomylonitic or brecciated rocks. The contact between the mylonite and protomylonite, or between the cataclasite and brecciated rocks, is usually irregular and often can only be arbitrarily placed. In cataclastic rocks the contact is often displaced by minor faults, or shows embayments and protrusions. In mylonitic rocks the transition is gradational and the zone of gradation may vary in width. Within the deformed region of the wall rock, movement on the fault is also accompanied by populations of minor shear zones or arrays of mesoscopic faults that may extend for hundreds of meters away from the fault (Wojtal 1986). This deformed region has been referred to as a "transition zone" (Yonkee 1991), a "damage zone" (Evans 1991) or, simply as a "protomylonite" (Sibson 1977) in mylonitic rocks. In this paper we refer to the major fault zone and the deformed hanging wall and footwall rocks together as the fault related deformation zone (FRDZ). The contact between the FRDZ and undeformed hanging wall and footwall rocks is also typically irregular, and must be defined according to specific meso- or microscopic evidence for each fault exposure studied. This paper focuses on deformation within the FRDZ in the

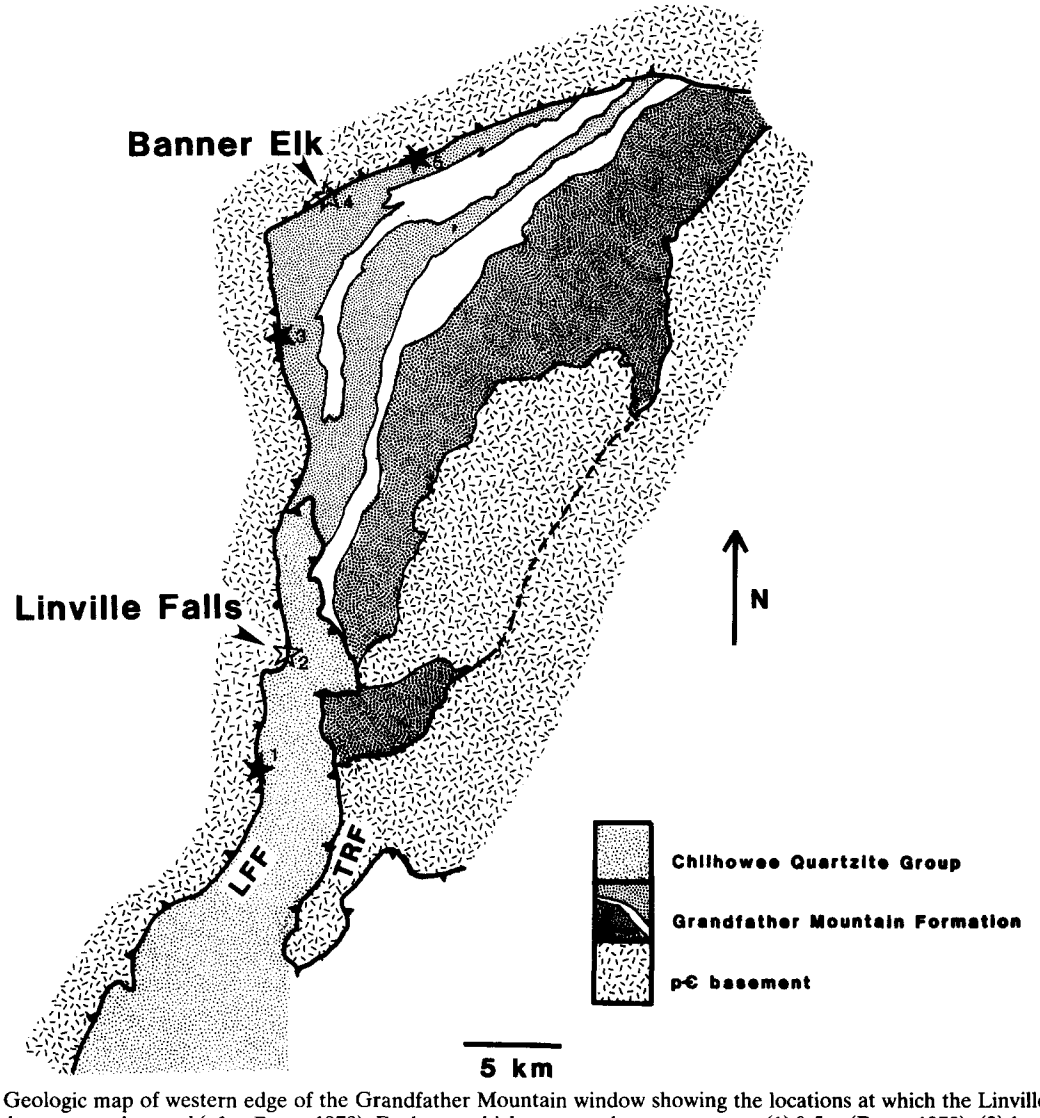

Fig. 2. Geologic map of western edge of the Grandfather Mountain window showing the locations at which the Linville Falls fault zone was observed (after Boyer 1978). Fault zone thicknesses at the exposure are: (1) 0.5 m (Boyer 1978); (2) 1 m; (3) approximately 60 m; (4) 60 m; (5) approximately 100 m. (2) and (4) are locations chosen for detailed study. LFF = Linville Falls fault; TRF = Tablerock fault.

hanging wall of the Linville Falls fault, and assumes that the mylonites studied were derived from the hanging wall. Our argument for this assumption, together with a brief description of the footwall deformation, is discussed in a later section.

Along the Linville Falls fault, deformation is characterized by ductile behavior with associated retrograde greenschist metamorphism giving rise to mylonites (fault zone) and protomylonites (within the rest of the FRDZ). In the northern segment of the fault, over a distance of 9 km, the fault zone mylonite thickness varies from at least 60 m to over 100 m at three locations where it can be observed (Fig. 2). In the southern segment, at two locations 6 km apart, the fault zone mylonite thickness is only 0.5–1 m. Two exposures, one along each segment of the fault, were chosen for detailed study; the mylonites are particularly well exposed at both these exposures allowing us to compare deformation styles between the two segments. The best exposure along the northern segment is at Banner Elk and is referred to as the Banner Elk exposure; the best exposure along the southern segment is at Linville Falls and is referred to as the Linville Falls exposure (Fig. 2). The two exposures are approximately 20 km apart along the strike of the Linville Falls fault. The following section describes the fault zone mineralogy and microstructure at the two locations studied.

MICROSTRUCTURES

Linville Falls exposure

The FRDZ at Linville Falls exhibits an approximately 1 m thick quartz–mica mylonite at the contact between the hanging wall gneiss and footwall Chilhowee quartzite. The hanging wall rocks adjacent to the mylonite are protomylonites showing evidence for retrograde alteration of the feldspar to 7–10 m above the mylonite zone, marking the top boundary of the FRDZ within the hanging wall; the zone also contains minor shear zones. Above this zone, alteration of feldspar is not observed.

The protolith at Linville Falls, as determined from a sample 50 m above the mylonite zone, is an alkali granite gneiss composed of 59% perthite and K-feldspar, 39% quartz, with minor amounts of muscovite, biotite, titanite, ilmenite, magnetite and garnet. The feldspar in the protolith is 25% K-feldspar and 75% perthite, as determined by optical analysis on thin sections stained for K and Na and confirmed by scanning electron microscope (SEM) energy dispersive analyses of X-rays (EDAX). These analyses indicate that the perthite in the protolith is Ab_{55} Or_{45} and the K-feldspar is Or_{100}. The protolith shows a coarse gneissic fabric. Intragranular fractures within the feldspars filled with recrystallized quartz are evidence of weak deformation beyond the FRDZ (Fig. 3a).

Approximately 3 m above the mylonite zone, a foliation is defined by quartz ribbons composed of dynamically recrystallized grains and thin (5–10 μm) strands of muscovite (Fig. 3b). The feldspars contain no perthite; the compositions of all remaining feldspar range from Or_{97} to Or_{99}. The modal percentage of feldspar drops from 59% in the protolith to 8% at 3 m above the mylonite zone. Also, modal abundances of muscovite and quartz increase from <1 to 27% and from 39 to 60%, respectively (Fig. 5a).

At a distance of 0.6 m above the mylonite zone the feldspar fragments are less angular, and are surrounded by muscovite, opaques, and some quartz (Fig. 3c). The growth of aligned muscovite and quartz between fragments indicates extension between feldspar fragments pulled apart after cracking. Quartz augen show subgrain and new grain development in a core and mantle structure, and asymmetric tails of mica, quartz and opaques appear around the feldspar and quartz augen.

At the outer boundary of the mylonite zone the modal percentage of feldspar in the rocks drops from 10 to 1.5%, and the percentage of muscovite increases from 34 to 80%. The modal percentage of quartz, on the other hand, changes its trend and drops from 39 to 19% (Fig. 5a). Bands 5–6 mm thick of strongly foliated and often crenulated mica and fine-grained quartz alternate with 3–4 mm thick bands of quartz and feldspar augen and opaque grains in a mica and quartz matrix. Many feldspar augen and some quartz augen are fractured (Fig. 3d). In the center of the mylonite zone, quartz and feldspar bands are fewer in number and thinner. The mylonite consists predominantly of strongly foliated muscovite.

Grain size is an important variable in fault zone deformation and the formation of a mylonite generally involves a reduction in grain size. We discuss grain size distribution data in this paper in addition to trends of mean grain size as this gives additional information about deformation behavior along a fault zone. Mean grain sizes and grain size distributions were determined by a lineal analysis using an integrating stage. We measured the chord lengths of each grain intersected in transects across the thin section (Mitra 1978). We completed four transects per thin section along lines parallel, perpendicular, and at ± 45° to the foliation. Grain size distributions were calculated using Spektor's chord analysis assuming a polydispersed system of spheres (Underwood 1970, p. 126).

Grain size distributions for quartz for each sample exhibit a log-normal distribution, and the distributions are unimodal (Fig. 6a). The feldspar grain size distributions are also generally logarithmic, but not unimodal (Fig. 6b). The distributions for most samples reveal one high peak at 20 μm and several shorter peaks at larger grain sizes. Approaching the center of the mylonite zone there is a general decrease in the height of peaks at grain sizes greater than 50 μm. Because the grain size distributions are logarithmic the following discussion uses geometric mean grain size which represents the value with the greatest frequency of grains.

Comparing mean grain sizes of protolith grains with mylonite grains (Fig. 5b) indicates a slight reduction in the grain size of the quartz (from 30 to 20 μm). The feldspar grain size drops from 110 to 70 μm at the boundary between the protolith and the FRDZ, and again at the top of the mylonite zone to 30 μm. These changes coincide with the points where the modal percentages of feldspar in the rock decrease.

The changes in modal composition across the fault zone at Linville Falls reflect gross chemical changes which are also apparent in whole rock analyses (Fig. 5c). There is a sharp decrease in the proportion of silica within the mylonite zone, and a corresponding increase in Al_2O_3, K_2O and Fe_2O_3. Many trace elements (Rb, V, Y, Cr) show a relative increase within the mylonite zone (Fig. 5d). The mineral reactions that are observed in the FRDZ (described in a later section) indicate open system behavior.

Banner Elk exposure

At the Banner Elk exposure a 60 m thick exposure of hanging wall quartz–mica mylonite is juxtaposed against footwall arkoses of the Grandfather Mountain Formation. A slice of quartzite, approximately 1.5 m wide, crops out 40 m above the contact with the footwall arkose; such tectonic slices of quartzite occur frequently within the Linville Falls fault zone (Bryant & Reed 1970). The protolith of the mylonitic rocks (Fig. 4a), estimated from an undeformed sample about 500 m above the fault zone, is a quartz diorite gneiss containing 59% plagioclase feldspar, 21% quartz, 13% biotite and trace amounts of muscovite. The feldspar consists of albite as the main phase with anorthite exsolution and alteration to muscovite within the grains (determined by SEM EDAX analyses) in approximately equal, but minor, amounts.

No feldspar remains in the mylonitic rocks of this fault zone exposure. No general changes or trends in textures, modal composition, mean grain size or chemical data were observed across the mylonite zone, although minor changes do occur within the vicinity of the quartzite slice (Figs. 5e–h). Comparing the modal composition of the protolith with the average modal composition of the mylonites indicates an increase in the proportions of

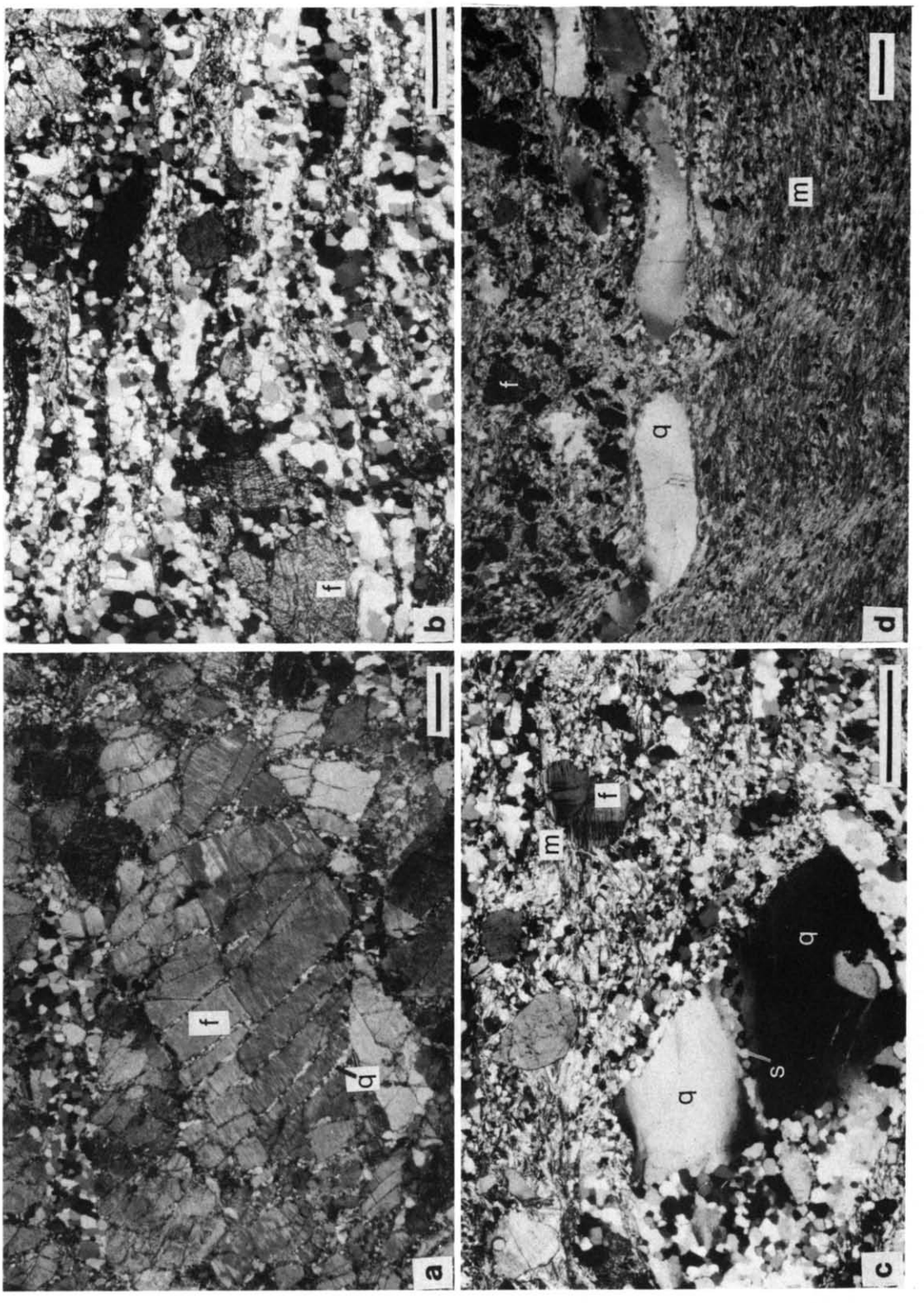

Fig. 3. Microstructures observed in rocks at the Linville Falls exposure. All sections are normal to the foliation and parallel to the lineation. (a) Protolith granite-gneiss. Feldspar is fractured and fractures are filled with recrystallized quartz. (b) 3 m above the mylonite zone. Foliation defined by quartz ribbons of recrystallized quartz and thin strands of muscovite; feldspar grains show fracturing. (c) 0.6 m above the mylonite zone. Alteration of feldspar suggested by muscovite and some quartz around feldspar fragments and the rounded shape of feldspar fragments. Quartz augen show undulose extinction and the development of subgrains and new grains. (d) Outer boundary of the mylonite zone. Band of strongly foliated and crenulated mica below band of opaques and quartz and feldspar augen in a fine-grained quartz and mica matrix. Quartz augen are fractured. f = feldspar, q = quartz, s = quartz subgrains, m = mica. Crossed polarizers. Scale bars = 0.5 mm.

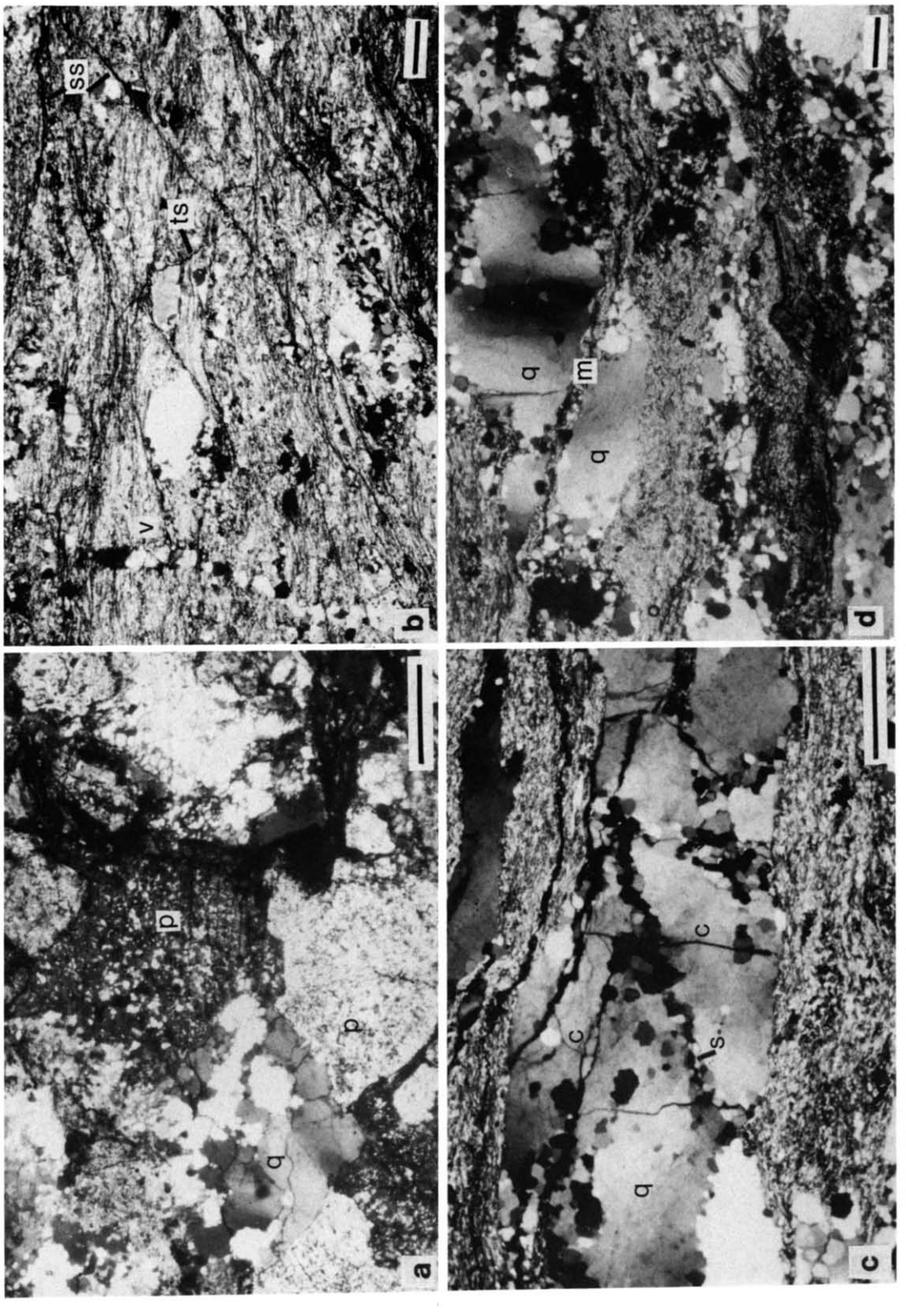

Fig. 4. Microstructures observed in rocks at the Banner Elk exposure. All sections are normal to the foliation and parallel to the lineation. (a) Protolith quartz–diorite gneiss showing coarse plagioclase grains and quartz. (b) Foliation defined by elongated quartz augen and the alignment of muscovite grains. Solution seams (ss) oblique and parallel to the foliation act as slip surfaces; seams perpendicular to the foliation are toothed stylolites (ts). Quartz vein (v) cross-cuts foliation. (c) Quartz augen showing undulose extinction, intragranular cracks (c), and recrystallization (subgrains) at grain boundaries and along cracks (s). (d) Fractured quartz augen. Mica infilling a fracture and separating fragments. p = plagioclase feldspar, q = quartz, m = mica. Crossed polarizers. Scale bars = 0.5 mm.

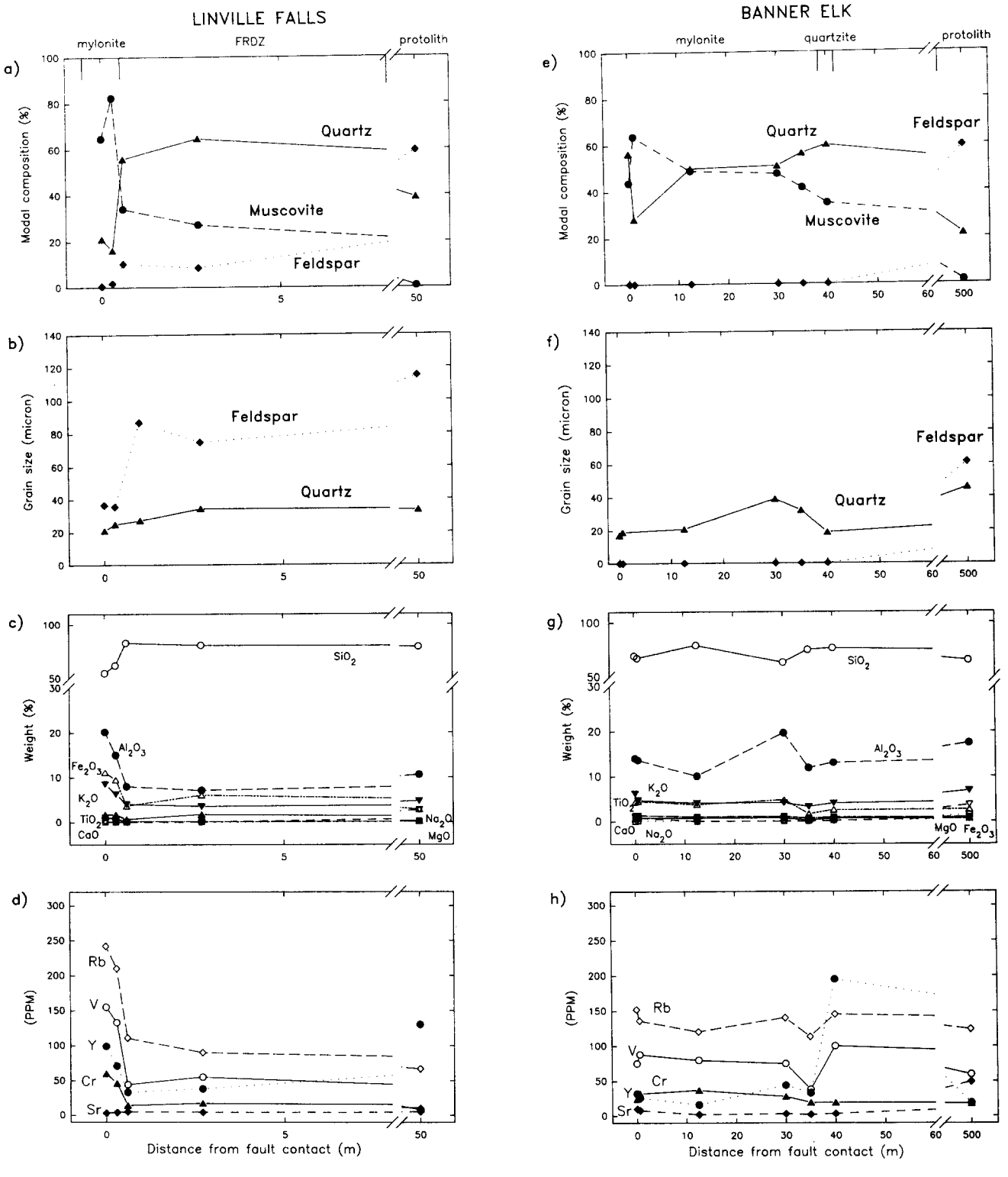

Fig. 5. Modal composition, geometric mean grain-size, major element and trace element abundance data for the Linville Falls exposure (a–d) and the Banner Elk exposure (e–h). Horizontal axis indicates perpendicular distance from the hanging wall (hw)–footwall (fw) contact (at 0 m) for all plots. At Linville Falls (a–d) the mylonite zone is 1 m wide, but adjacent rocks show deformation associated with faulting to 8–10 m from the hw–fw contact (FRDZ). At Banner Elk the mylonite is at least 60 m wide. A tectonic slice of quartzite (1.5 m wide) appears at 40 m from the hw–fw contact. (e) Note that there is no feldspar within the mylonite zone, and that local loss of quartz occurs 0.6 m from the hw–fw contact.

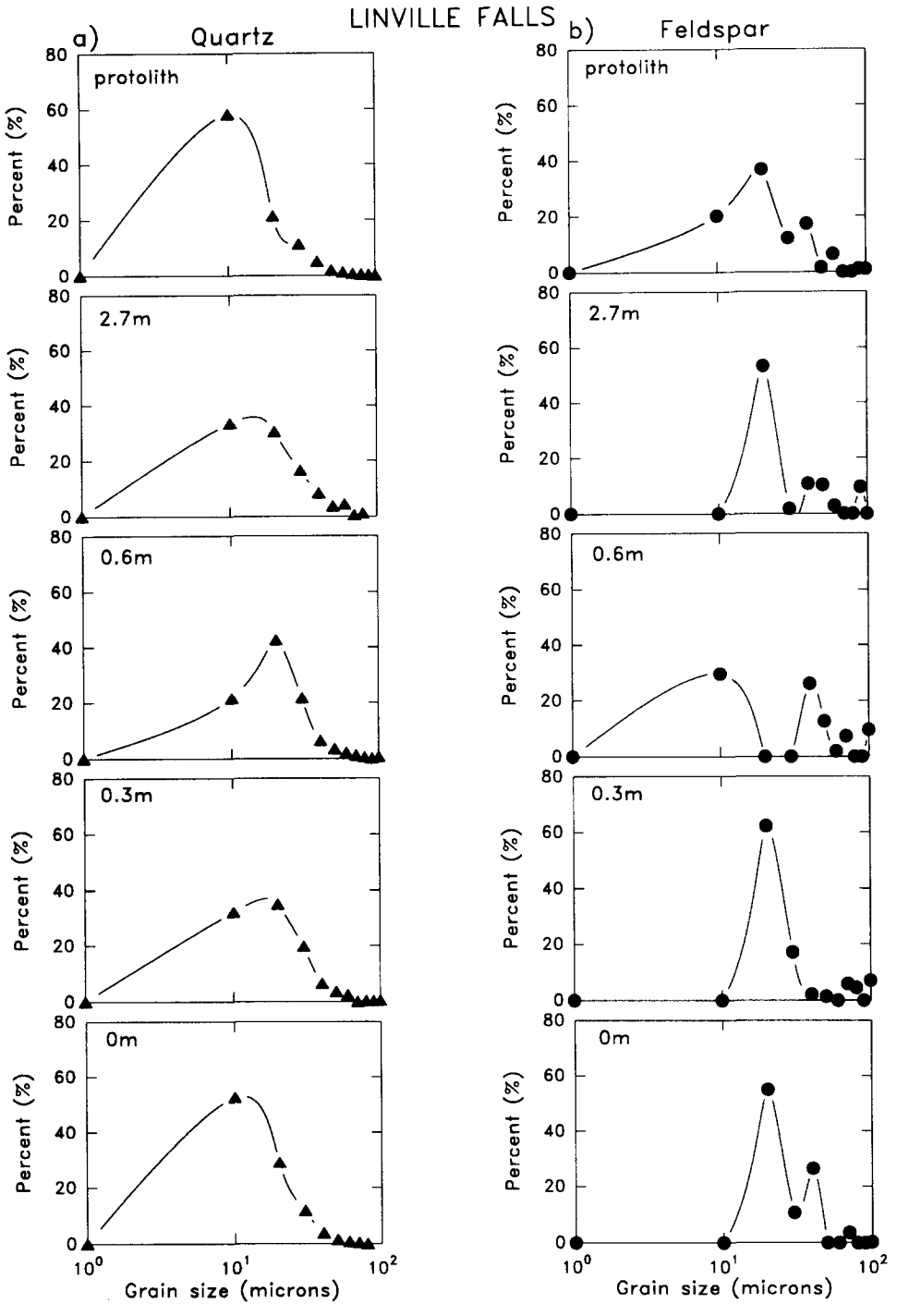

Fig. 6. Grain size distribution data for the Linville Falls exposure. Grain size interval is 10 μm for both minerals, plotted on a logarithmic scale. Distance from the mylonite zone indicated in top left corner of each graph. (a) Quartz grain size distribution. (b) Feldspar grain size distribution.

quartz from 21 to 50%, and muscovite from 1.4 to 44%. Compositions of individual samples are shown in Fig. 5(e). The quartz grain size distributions within the mylonite zone at Banner Elk follow a log-normal distribution and are unimodal (Fig. 7). Quartz augen exhibit subgrain and new grain development and the mean grain size of the quartz is reduced from 60 μm in the protolith to 24 μm in the mylonite.

The foliation in these mylonite rocks is defined by elongated quartz augen, recrystallized quartz ribbons and the aligned muscovite grains (Fig. 4b). Asymmetric tails of quartz or quartz and muscovite are common around the quartz augen. The quartz augen also contain many intragranular cracks. Often the cracks are lined with subgrains and new grains of quartz, particularly those cracks that are parallel or slightly oblique to the foliation (Fig. 4c). Fractured augen are often offset, and fragments are pulled apart (Fig. 4d). Thin recrystallized quartz veins (<10 μm wide) cut across the foliation at high angles; because the veins have not undergone significant amounts of rotation in this zone of high shearing they probably developed late in the deformation history (Fig. 4b). Some veins are offset by mica-rich matrix, suggesting that the matrix was still deforming in a ductile manner after the development of the veins. Within the mica-rich zones, solution seams cross-

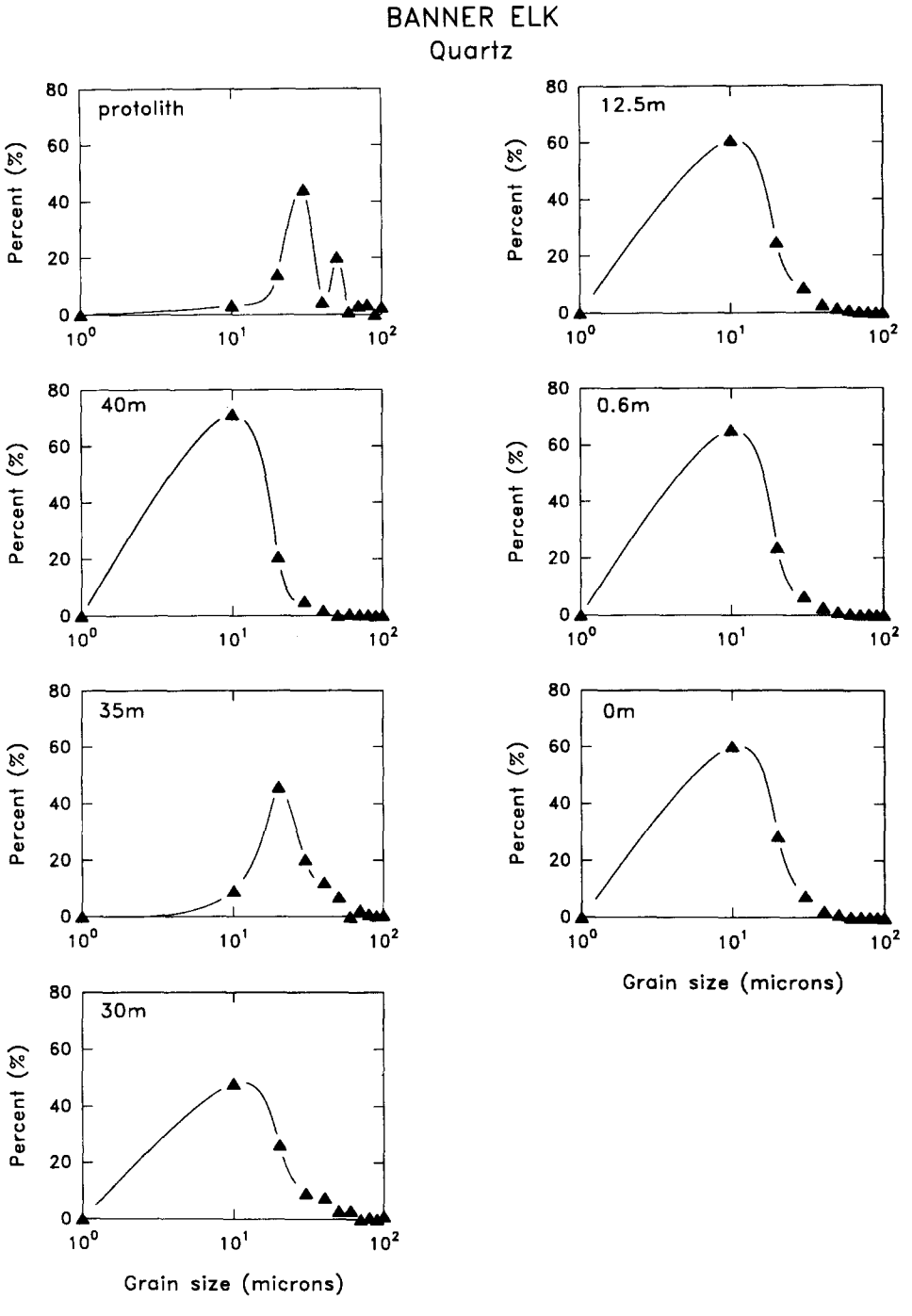

Fig. 7. Quartz grain size distribution data for the Banner Elk exposure. Grain size interval is 10 μm plotted on a logarithmic scale. Distance from the mylonite zone is indicated in top left corner of each graph.

cut the mylonitic foliation, indicating that solution occurred later in the deformation. The seams that are perpendicular to the foliation are toothed stylolites; those parallel and oblique to the foliation are planar or curviplanar (Fig. 4b). Transgranular cracks and microfaults appear in the quartz–mica mylonite within 8 m of the contact of the basement with the footwall arkose.

INTERPRETATION OF MICROSTRUCTURES

Linville Falls exposure

Deformation along the fault at the Linville Falls exposure occurred primarily by fracturing of feldspar, the alteration of feldspar to muscovite and quartz, and the continued grain size reduction of quartz by dynamic recrystallization of quartz augen. The alteration of feldspar is supported by modal composition data. The decreases in the modal amounts of feldspar from the protolith to the FRDZ coincide with increases in the proportions of quartz and mica within the FRDZ. The increasing proportions of quartz and mica suggest that reaction softening (White & Knipe 1978) contributed to the deformation. Slip along the (001) planes of the increasingly prevalent aligned mica grains allowed for an increased strain rate resulting in the further fracturing of the feldspar and some quartz augen due to localized stress build-up at the grain boundaries (Mitra 1978).

The reduction in mean grain size of feldspar further supports this interpretation. A heterogeneous grain size distribution (Fig. 6b) is common where grain size reduction takes place by fracturing (Schmid 1983). The trends are complicated, probably reflecting that the grain size reduction took place by a combination of fracturing and alteration to quartz and mica. The sharp unimodal size distributions of the quartz grains (Fig. 6a) probably indicate that a steady-state recrystallized quartz grain size had been reached within the mylonite zone.

The microstructures and the trends in modal composition suggest that the following feldspar breakdown reactions occurred:

$$\underset{\text{albite}}{2NaAlSi_3O_8} + \underset{\text{K-feldspar}}{KAlSi_3O_8} + 2H^+ = \underset{\text{muscovite}}{KAl_3Si_3O_{10}(OH)_2} + \underset{\text{quartz}}{6SiO_2} + 2Na^+ \quad (1)$$

or

$$\underset{\text{K-feldspar}}{1.5KAlSi_3O_8} + H^+ = \underset{\text{muscovite}}{0.5KAl_3Si_3O_{10}(OH)_2} + \underset{\text{quartz–silica (aq)}}{3SiO_2} + K^+. \quad (2)$$

It is important to note that the reactions require an increase in the proportion of quartz as well as muscovite with the alteration of feldspar. Figure 5(a) shows, however, that while there is an increase in the proportion of quartz from the protolith to the FRDZ, there is a sharp decrease in the proportion of quartz within the mylonite zone. Also, although within the FRDZ, both quartz and muscovite are observed around the edges and along fractures within the feldspar augen, it is much more common for only muscovite to appear surrounding the feldspar augen within the mylonite zone. This suggests that quartz was dissolved and transported out of the system during or after the feldspar-breakdown reaction, leaving a muscovite-rich rock.

Dissolution of silica during the feldspar-breakdown reaction has been noted by other authors (e.g. Losh 1989, O'Hara 1990). At Linville Falls, however, dissolution involved not only silica from the breakdown of the feldspar, but also protolith quartz, as indicated by the lower proportion of quartz and SiO_2 in the mylonite than in the protolith. We do find an initial increase in the modal percent of quartz in the outer portion of the FRDZ, which presumably resulted from the crystallization of quartz from the breakdown of the feldspar. The paucity of SiO_2 within the mylonite zone indicates that the quartz dissolution occurred primarily along the narrow mylonite zone observed at the contact with the footwall.

Banner Elk exposure

At Banner Elk, the alteration of feldspar is also indicated by the loss of feldspar and the increases in the proportions of quartz and muscovite. The grain size of the quartz is reduced by dynamic recrystallization and presumably by the crystallization of fine-grained quartz from feldspar breakdown. Reaction softening (White & Knipe 1978), indicated by the alteration of feldspar to quartz and muscovite, thus contributed to the deformation. Slip of the mica served as a softening mechanism allowing for continued motion along the fault, offsetting veins and augen. In addition, the fine grain size of the recrystallized quartz may have contributed to a switch in the dominant deformation mechanism of the quartz from dynamic recrystallization to diffusion processes (White 1976, Mitra 1978), indicated by pressure shadows adjacent to quartz augen, further contributing to the ductile flow (Wojtal & Mitra 1986). As at Linville Falls, the ductile flow of the mica and quartz may have allowed for an increased strain rate resulting in fracturing of the quartz augen. One sample 1 m from the footwall exhibited less SiO_2 than other samples from the mylonitic rocks (Fig. 5e) perhaps indicating that quartz dissolution occurred only locally at Banner Elk.

The transgranular cracks and microfaults that appear within the hanging wall close to the contact with the footwall arkose (which exhibits cataclastic deformation) suggest that late in the deformation the hanging wall moved up into the elastico-frictional regime (Sibson 1977). These features are not pervasive, however, and probably do not account for much of the deformation.

COMPARISON OF THE TWO EXPOSURES

The quartz–mica microstructures within the mylonite zone at the two exposures show similar deformation features. The quartz has deformed by dynamic recrystallization. The feldspar has altered to muscovite and quartz so that little or no feldspar remains, and the proportion of muscovite has increased from the protolith to the mylonite at both exposures. The proportion of quartz in the protolith at Banner Elk (21.4%) is lower than at Linville Falls (39.0%). Yet at Banner Elk the ratio of quartz to muscovite (1.3) in the mylonite zone is significantly higher than at Linville Falls (0.25). Also, there is a greater volume of altered rock (quartz–mica mylonite with little or no feldspar remaining) at Banner Elk than at Linville Falls (>60 m thickness vs 1 m thickness). An important difference is the type of feldspar in the protoliths at the two exposures: K-feldspar and perthite at Linville Falls, plagioclase at Banner Elk. In addition, the behaviors of major and trace elements at the two exposures differ. There is a marked increase in many trace elements and major oxides within the mylonite zone at Linville Falls, and a decrease in silica. At Banner Elk there do not appear to be significant changes in element concentrations between the protolith and the mylonite.

The differences observed between the two fault exposures suggest possible explanations for the variations. First, the decrease in quartz, and the sharp decrease in Si within the mylonite zone suggest that volume loss may have occurred at Linville Falls resulting in a thinning of the fault zone there. The increased concentration of

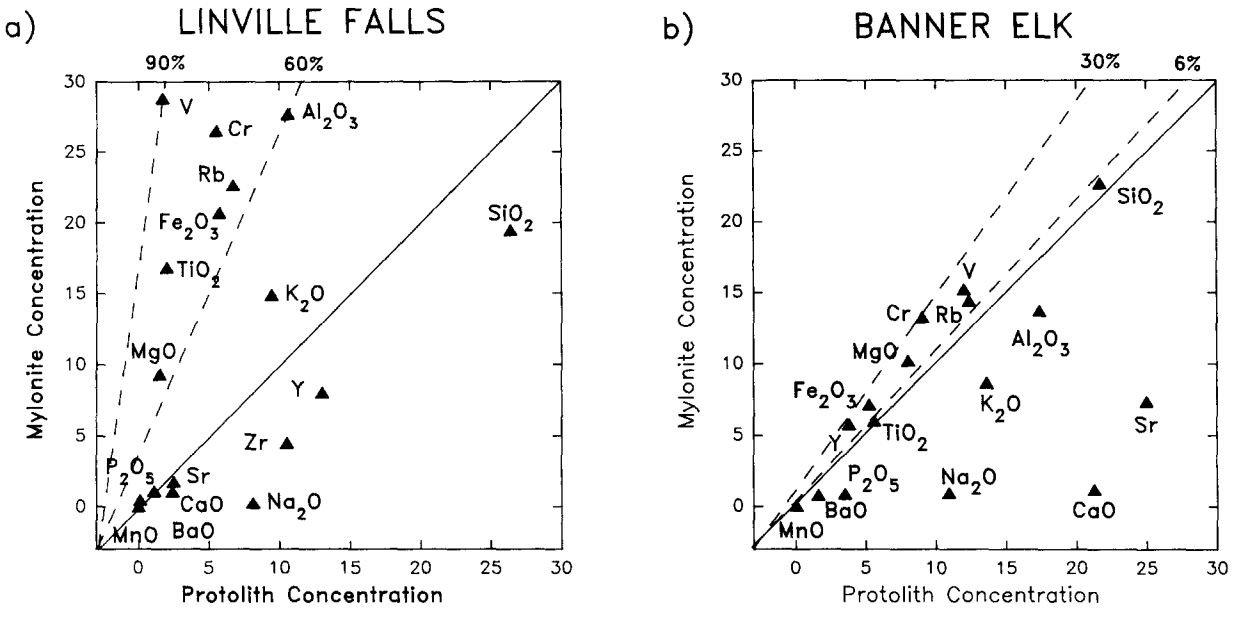

Fig. 8. Isocon diagrams (after Grant 1986 and O'Hara 1988) comparing trace element and major oxide concentrations within the mylonites to those within the protoliths. Protolith concentrations are on the horizontal axes; mylonite concentrations are on the vertical axes. Values used for mylonite concentrations are mean values of two samples closest to the hw–fw contacts at each exposure. Element concentrations are scaled to 0–30 wt % or ppm. The solid line represents a 1:1 correspondence between mylonite and protolith concentrations. The mylonite has become enriched in those elements above the solid line and depleted in elements below the line. Dashed lines indicate minimum and maximum estimates of volume loss based on concentrations of immobile elements. (a) Data for the Linville Falls exposure. (b) Data for the Banner Elk exposure.

relatively insoluble elements (Figs. 5c&d) further supports the possibility of volume loss. Second, the larger volume of altered rocks observed at the Banner Elk exposure suggests that more fluids may have infiltrated the fault zone at Banner Elk, altering the feldspar to muscovite and quartz over a larger thickness of rock. These possibilities are discussed in following sections.

VOLUME LOSS

To investigate the possibility of volume loss, major oxide and trace element concentrations were plotted on isocon diagrams (Grant 1986) (Fig. 8). These diagrams compare element concentrations in the altered rock (mylonite) to concentrations in the original rock (protolith). A 1:1 correspondence between altered rock and original concentrations would indicate that an element had not been depleted or augmented during deformation.

At Linville Falls enrichment is seen in the mylonite in the following major oxides (Fig. 8a): Fe_2O_3, TiO_2, MgO, Al_2O_3, K_2O, BaO and MnO. BaO and MnO are present in such low amounts that their significance can be discounted. Al_2O_3 is relatively immobile (Hem 1978), as are MgO and TiO_2 (Correns 1978), although Al mobility may be important in deforming rocks (Dipple *et al.* 1990). Trace elements V and Cr, also considered relatively immobile, are also enriched in the mylonite. V, which may have substituted for Al or K in the feldspars, could have moved into the forming muscovite. Cr most likely remained in the insoluble magnetite and ilmenite. It is unlikely that the enrichment of these elements resulted from their movement into the system. Rather, we infer that the enrichment of these elements is the result of the depletion of SiO_2 and other soluble oxides such as Na_2O and CaO.

From this inference, it is possible to estimate the volume loss of the system from the concentration of the relatively immobile elements (Kerrich *et al.* 1980, O'Hara 1988). As there is a wide range of variability in the enrichment of these elements, and in their partitioning behaviors, it is only possible to establish a range for the possible volume loss. We used the enrichment of Al_2O_3 as a lower bound, and the enrichment of V as an upper bound to establish two isocons at Linville Falls. The slope of the isocon determines the volume loss according to the equation (O'Hara 1988):

$$C_i/C_o = 1/(1 - V),$$

where C_i represents the concentration of the element in the deformed state, C_o is the concentration of the element in the original state, and V represents the volume loss. A lower bound of 60% and an upper bound of 90% volume loss are suggested from the data.

At Banner Elk elements appear to have behaved quite differently (Fig. 8b). The enrichment of immobile elements in the mylonite is not as marked as seen at Linville Falls, although a small amount of enrichment is seen, particularly in MgO, TiO_2, Cr, V and Rb. Using TiO_2 as a lower bound and Cr as an upper bound, volume loss at Banner Elk is estimated at 6–30%, substantially lower than the range suggested at Linville Falls.

VOLUME OF FLUIDS

The fluid–rock ratios and the total volume of fluids infiltrating the fault zone at the two exposures may also have influenced the structure of the fault zone. The fluid–rock ratio may be related to volume loss along the mylonite zone. Also, more fluids may have infiltrated the fault zone at Banner Elk than at Linville Falls, resulting in the greater thickness of altered rocks seen there. To compare fluid–rock ratios and the total volumes of fluid that infiltrated the Linville Falls fault at the two exposures, an estimation was accomplished in three steps. First, to determine the amount of silica lost at each exposure we used Gresens's (1967) equation relating rock density and volume loss with chemical changes during deformation and metamorphism. Second, we estimated fluid–rock ratios by determining the amount of fluid necessary to cause the observed loss of silica, assuming mid-greenschist grade conditions; and, third, to compare the volume of fluids that infiltrated the fault zone at each exposure, we multiplied the fluid–rock ratios by a column of rock of unit cross-sectional area and height equal to the thickness at each exposure prior to volume loss.

Gresens's (1967) equation allows gains and losses of mobile elements, such as SiO_2, to be calculated once volume change has been established. The equation relates rock densities (calculated from modal mineralogy of the rocks) of the protolith and altered rocks [2.67 g cm^{-3} (protolith) and 2.80 g cm^{-3} (mylonite) at Linville Falls, and 2.69 g cm^{-3} (protolith) and 2.72 g cm^{-3} (mylonite) at Banner Elk] and volume loss with chemical changes during deformation. Mean values for volume loss at each exposure (75 and 20% at Linville Falls and Banner Elk, respectively) were used to write the following equations.

Linville Falls:

$$100\text{ g gneiss} - 63.9\text{ g } SiO_2 - 3.3\text{ g } Al_2O_3 - 2.8\text{ g } K_2O - 2.7\text{ g } Na_2O - 0.2\text{ g } Fe_2O_3 - 0.2\text{ g CaO} - 0.2\text{ g } P_2O_5 = 26.6\text{ g mylonite} + 0.2\text{ g } TiO_2 + 0.1\text{ g MgO}.$$

Banner Elk:

$$100\text{ g gneiss} - 7.3\text{ g } SiO_2 - 6.3\text{ g } Al_2O_3 - 3.4\text{ g } Na_2O - 3.3\text{ g } K_2O - 1.3\text{ g CaO} - 0.3\text{ g } P_2O_5 = 78\text{ g mylonite} + 0.02\text{ g MgO} + 0.3\text{ g } Fe_2O_3.$$

Fluid–rock ratios were determined using the losses of SiO_2 and a quartz solubility for mid-greenschist grade (400°C, 4 kb) of 0.3 wt% (Currie 1968).

Many assumptions are necessary in estimating the fluid–rock ratio. First, lithologic variations in the parent rock may lead to under- or overestimation of the amount of silica dissolved. Underestimation of the fluid–rock ratio may also result from the assumption that once the fluids entered the fault zone they became saturated with silica. The fluid flux may not have allowed the time necessary for saturation. In addition, while the prior concentration of silica in the infiltrating fluids will limit the amount of silica dissolution that can take place, high salinity and high pH may increase the solubility of quartz

Table 1. Fluid–rock ratios and volumes of fluid infiltrating the fault zone at Linville Falls and Banner Elk assuming a range of values for silica saturation of fluids. Values for volume losses are based on the ranges of volume loss estimated for each exposure

Silica saturation (%)	Linville Falls Fluid–rock ratio	Linville Falls Volume fluid (m^3)	Banner Elk Fluid–rock ratio	Banner Elk Volume fluid (m^3)
	60% volume loss		10% volume loss	
0	182	4.6×10^2	0.1	6.7
50	365	9.1×10^2	0.2	1.3×10^1
90	1825	4.6×10^3	1	6.7×10^1
	75% volume loss		20% volume loss	
0	213	8.5×10^2	24	1.8×10^3
50	426	1.7×10^3	48	3.6×10^3
90	2130	8.5×10^3	242	1.8×10^4
	90% volume loss		30% volume loss	
0	244	2.4×10^3	48	4.0×10^3
50	487	4.9×10^3	96	8.2×10^3
90	2436	2.4×10^4	483	4.1×10^4

(Fournier 1985). Previous discussions of fluid–rock ratios have assumed 100% undersaturation as the prior concentration of infiltrating fluids (e.g. Losh 1989), or, a range of saturation (50 and 90%, O'Hara 1988). Sinha *et al.* (1986) have determined the degree of saturation possible assuming a change in temperature resulting from the migration of fluids up the fault zone. The method chosen influences the estimated fluid–rock ratio significantly, by more than an order of magnitude in some instances (e.g. O'Hara 1988, this study). We have no data on the silica concentration of the infiltrating fluids prior to entering the fault zone, or the fluid flux. Thus we have estimated the fluid–rock ratio over a wide range of saturation levels and over the ranges estimated for volume loss at each exposure (Table 1). This will allow some degree of comparison with estimates made by other workers.

Comparison between the two exposures under any set of the given conditions shows that the fluid–rock ratio at Linville Falls is at least an order of magnitude greater than at Banner Elk. Most of the assumptions described above lead to an underestimation of the fluid–rock ratio. Also, for fluids present in the host rocks a high degree of saturation with respect to quartz may be expected at greenschist grade temperatures (approximately 400°C) (Rimstidt & Barnes 1980). Therefore, an estimated fluid–rock ratio assuming that the infiltrating fluids were at least 90% saturated with quartz prior to entering the fault zone may be the most realistic. Assuming mean values for volume loss and that fluids were 90% saturated prior to entering the fault zone, fluid–rock ratios of 2130 at Linville Falls and 242 at Banner Elk are required to cause the silica depletions observed.

To estimate the volume of fluid that infiltrated the fault zone at the two exposures we multiplied the fluid–rock ratios by columns of rock with unit cross-sectional area and height equal to the thickness of the fault zone prior to deformation at the two exposures (Table 1).

Assuming mean volume losses and that fluids were 90% saturated with silica prior to entering the fault zone, we estimate 0.85×10^4 m^3 fluid infiltrated the fault at Linville Falls, and 1.8×10^4 m^3 at Banner Elk. Approximately twice as much fluid infiltrated the fault zone at Banner Elk as at Linville Falls, but the amounts are within the same order of magnitude.

DISCUSSION

Why is the structure of the fault zone different at the two exposures? At Linville Falls the fault zone is thin, has experienced significant volume loss and had a high fluid–rock ratio. The fault zone at Banner Elk is thick, has experienced very little volume loss and had a comparatively low fluid–rock ratio. In addition, a larger volume of fluid infiltrated the fault zone at Banner Elk than at Linville Falls. Although the lithologies of the hanging wall at both exposures are similar, the differences in feldspar mineralogy may have influenced the structure of the fault zone at the two exposures. At Linville Falls perthite (44%) and K-feldspar (15%) predominate, while at Banner Elk plagioclase feldspar (59%) predominates. At Banner Elk the plagioclase feldspar seen in the protolith has been completely altered to quartz and muscovite in the mylonite. At Linville Falls, the plagioclase in the perthite is not present in the mylonite or in the FRDZ. K-feldspar is still observed in the FRDZ, and in trace quantities within the mylonite zone.

The alteration of plagioclase appears to have occurred more readily than the alteration of K-feldspar. Within the northern Blue Ridge, the opposite sequence is seen: the proportion of K-feldspar is reduced before plagioclase feldspar in traverses approaching the center of basement shear zones (Mitra 1978). The composition of infiltrating fluids may influence the reaction that takes place. The alteration of feldspar to muscovite and quartz results in volume change and high permeability (Etheridge *et al.* 1983, 1984). The weak bonding between (001) planes in layer silicates results in higher porosity than in the strongly bonded framework silicates (Etheridge *et al.* 1983). Additionally, the alteration of feldspar combined with the grain size reduction of quartz create new grain boundaries further increasing permeability. This combined with increased porosity due to microcracking in feldspar and quartz grains may have given rise to an effective interconnected porosity, influencing permeability and fluid mobility (Etheridge *et al.* 1983). We suggest that along the Linville Falls fault zone, fluids were able to infiltrate a larger volume of rock at Banner Elk because the alteration of plagioclase occurred readily, creating new pathways for fluids. At Linville Falls the K-feldspar did not alter as readily as the plagioclase so that the infiltration of fluids was more difficult. As new infiltrating pathways were difficult to create, one zone was preferred, resulting in a thin zone with a very high fluid–rock ratio.

The fluid–rock ratio at Linville Falls is an order of magnitude higher than at Banner Elk. Locally, substantially more fluids passed through the thin zone at Linville Falls. This high fluid–rock ratio may have helped to accomplish the large volume loss estimated for Linville Falls as discussed previously. The fluids resulted in the alteration of feldspar, and reaction softening coupled with the dissolution of silica helped to localize the strain. Slip along mica cleavage planes then accommodated much of the strain along the thin zone.

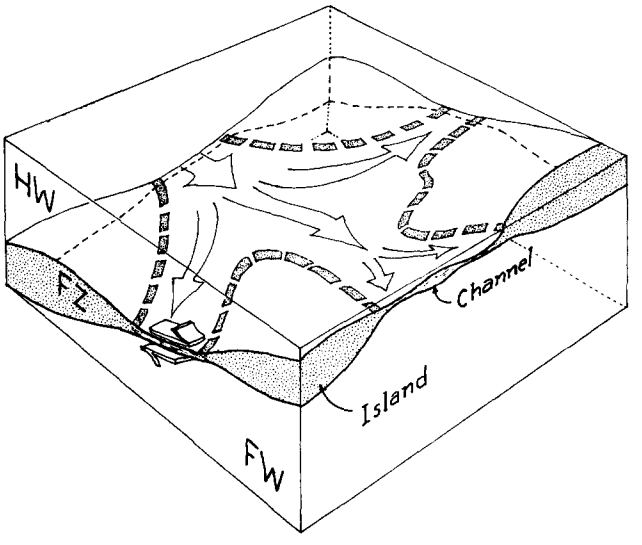

Fig. 9. Schematic sketch illustrating the island and channel structure of a fault zone (FZ).

At Banner Elk, however, the dissolution of the feldspar and precipitation of quartz and mica did not result in such a high degree of strain localization. Discussions on the initiation of shear zones suggest that metamorphic reactions may occur in the earliest stages of shear zone formation (Mitra 1978, Beach 1980). Vernon & Flood (1988) showed that the degree of localization of strain during greenschist grade regional metamorphism in granitoid rocks is dependent on the ratio of strong (e.g. feldspar) to weak (e.g. quartz and mica) minerals; as the ratio decreases, localization of strain is less likely. If the feldspar-breakdown reaction occurred over a great thickness at Banner Elk, a wide zone of weakness was created, and localization of the strain was not favored.

Variations in fluid flow along a fault zone may be considered somewhat analogous to the grain boundary model of islands and channels (Mott 1948, Raj & Chyung 1981), where the surface of contact between two grains consists of 'islands', thick regions of distorted structure with relatively good fit, separated by 'channels', thin zones of poor fit containing fluid. By analogy, a fault zone is a boundary between two sheets of rock. The regions of lower fluid flow along the fault zone are in essence, 'islands', thick deformed zones that allow fault zone fluids to infiltrate into surrounding rocks; regions of higher fluid flow are 'channels', thin zones that allow migration of fluid along the fault zone (Fig. 9). Fluids migrate preferentially through the channels, creating a three-dimensional network of higher fluid flow along portions of the fault zone. Along the Linville Falls fault,

the portion of the fault at the Linville Falls exposure may represent a channel, a thin zone with a high fluid–rock ratio; the portion of the fault exposed at Banner Elk may have served as an island—a thicker zone with low fluid–rock ratio. In this instance, more total fluids may have infiltrated the 'island', despite the higher fluid–rock ratio along the 'channel'.

The source of the fluids that infiltrated the fault zone is unknown, but probably had a large influence on the volume loss behavior. The fluids may be derived from surface waters that infiltrated down the fault zone. Surface waters would have low silica saturation, favoring a larger volume loss. Alternatively, the fluids may be derived from the dewatering of sedimentary rocks in the footwall. These fluids might be more highly saturated with silica, resulting in less volume loss. Our data do not allow us to distinguish between these two possibilities.

This discussion has concentrated on the changes occurring between the hanging wall rocks and the mylonitic fault rocks at both exposures. The footwall rocks were not discussed here for two reasons. First, the lithologies of the footwalls at the two exposures are significantly different from one another. At Linville Falls, the footwall is a quartzite, and contains predominantly clastic grains of quartz with some K-feldspar and mica. At Banner Elk the footwall is a poorly sorted arkosic sandstone, and contains angular to subrounded clastic grains of quartz, K-feldspar, and plagioclase in a groundmass of quartz, K-feldspar and mica. The proportion of mica varies a great deal at a mesoscopic (outcrop) scale near the FRDZ at Banner Elk. Second, the deformation styles of the footwall rocks at the two locations also differ substantially from one another. At Linville Falls the quartzite deformed like the hanging wall rocks at that location, in a ductile manner. Quartz deformed by dynamic recrystallization, and feldspar grains fractured and altered to quartz and mica. At Banner Elk, the footwall rocks exhibit both feldspar and quartz fragments deformed by fracturing. Feldspar also deformed by alteration to quartz and mica. There is no evidence for the dynamic recrystallization exhibited by quartz in the hanging wall rocks. The crystal-plastic microstructures in the hanging wall rocks at Banner Elk are overprinted by late stage cataclastic deformation. The contact between the hanging wall rocks and the cataclastically deformed footwall rocks is quite sharp, with 5–15 cm of very fine-grained strongly deformed rock. As the footwall rocks do not display evidence for earlier crystal-plastic deformation, the mylonitic rocks could not possibly have been derived from the footwall rocks now adjacent to the fault. The mylonites have clearly moved with the hanging wall rocks from some other location. It is therefore futile to compare the footwall rocks with the mylonitic fault rocks at this location.

At Linville Falls it is less clear whether the mylonite rocks observed were derived from the hanging wall or the footwall. Samples of the mylonite were collected from the center of the mylonite zone and the region of the mylonite adjacent to the hanging wall to lessen the possibility that they were derived from the footwall. In addition, it should be noted that if the mylonites were derived from the footwall quartzites, the depletion of silica within the mylonite relative to the footwall rocks would be even greater than that relative to the hanging wall. This would suggest an even higher value for the volume loss at the Linville Falls exposure.

CONCLUSIONS

The thickness of the Linville Falls fault zone varies over more than one order of magnitude at two distinct locations along the strike of the fault, separated by 20 km. The influences on this variation include: (1) significant volume loss at Linville Falls, predominantly by the dissolution of silica, contributed to a thinning of the fault zone there; (2) the exposure at Linville Falls experienced a higher fluid–rock ratio than the exposure at Banner Elk. Yet a greater volume of fluid may have infiltrated the fault zone at Banner Elk than at Linville Falls; and (3) the different feldspar mineralogy of the protoliths at the two fault exposures (plagioclase at Banner Elk and K-feldspar and perthite at Linville Falls) contributed to the different deformation behaviors observed at the two fault exposures. Plagioclase at Banner Elk altered to quartz and muscovite more readily than K-feldspar at Linville Falls, creating pathways for fluids over a thicker zone at Banner Elk. One thin zone, with a high fluid–rock ratio was preferred at Linville Falls.

Variations in fluid flow along a fault zone is analogous to the grain boundary model of islands and channels. Fluids may migrate preferentially through channels, creating a three-dimensional network of higher fluid flow along portions of the fault zone.

Acknowledgements—This research was supported by NSF grant EAR N005478 to G. Mitra, and by grants from the Geological Society of America and Sigma Xi to J. Newman. We thank S. Wojtal for a detailed review of an earlier draft of this paper, and K. O'Hara and an anonymous reviewer for their helpful comments

REFERENCES

Beach, A. 1980. Retrogressive metamorphic processes in shear zones with special reference to the Lewisian complex. *J. Struct. Geol.* **2**, 257–263.

Boyer, S. & Elliott, D. 1982. Thrust systems. *Bull. Am. Ass. Petrol. Geol.* **66**, 1196–1230.

Bryant, B. & Reed, J. C., Jr. 1970. Geology of the Grandfather Mountain Window and Vicinity, North Carolina and Tennessee. *Prof. Pap. U.S. Geol. Surv.* **615**.

Correns, C. W. 1978. Ti-behavior during weathering and alteration of rocks. In: *Handbook of Geochemistry* (edited by Wedepohl, K. H.), **II/2**, 22-G, 1–3.

Currie, K. L. 1968. On the solubility of albite in supercritical water in the range 400 to 600 C and 750 to 3500 bars. *Am. J. Sci.* **266**, 321–341.

Dipple, G. M., Wintsch, R. P. & Andrews, M. S. 1990. Identification of the scales of differential element mobility in a ductile fault zone. *J. metamorph. Geol.* **8**, 645–661.

Evans, J. P. 1991. Evolution of the hydrologic character of faults in crystalline rocks. *Geol. Soc. Am. Abs. w. Prog.* **23**, A103.

Etheridge, M. A., Wall, V. J., Cox, S. F. & Vernon, R. H. 1984. High fluid pressures during regional metamorphism and deformation: Implications for mass transport and deformation mechanisms. *J. geophys. Res.* **89**, 4344–4358.

Etheridge, M. A., Wall, V. J. & Vernon, R. H. 1983. The role of the fluid phase during regional metamorphism and deformation. *J. metamorph. Geol.* **1**, 205–226.

Fournier, R. O. 1985. The behavior of silica in hydrothermal systems. In: *Geology and Geochemistry of Epithermal Systems* (edited by Berger, B. R. & Bethke, P. M.). *Rev. Econ. Geol.* **2**, 45–61.

Gibson, R. G. & Gray, D. R. 1985. Ductile-to-brittle transition in shear during thrust sheet emplacement, Southern Appalachian thrust belt. *J. Struct. Geol.* **7**, 513–525.

Grant, J. A. 1986. The isocon diagram—A simple solution to Gresens' equation for metasomatic alteration. *Econ. Geol.* **81**, 1976–1982.

Gresens, R. L. 1967. Composition–volume relationships of metasomatism. *Chem. Geol.* **2**, 47–65.

Hem, J. D. 1978. Al—behavior during weathering and alteration of rocks. In: *Handbook of Geochemistry* (edited by Wedepohl, K. H.), **II/1**, 13-G,1.

Kerrich, R., Allison, I., Barnett, R. L., Moss, S. & Starkey, J. 1980. Microstructural and chemical transformations accompanying deformation of granite in a shear zone at Mieville, Switzerland; with implications for stress corrosion cracking and superplastic flow. *Contr. Miner. Petrol.* **73**: 221–242.

Losh, S. 1989. Fluid–rock interaction in an evolving ductile shear zone and across the brittle–ductile transition, Central Pyrenees, France. *Am. J. Sci.* **289**, 600–648.

Mitra, G. 1978. Ductile deformation zones and mylonites: The mechanical processes involved in the deformation of crystalline basement rocks. *Am. J. Sci.* **278**, 1057–1084.

Mitra, G. 1984. Brittle to ductile transition due to large strains along the White Rock thrust, Wind River mountains, Wyoming. *J. Struct. Geol.* **6**, 51–61.

Mott, N. F. 1948. Slip at grain boundaries and grain growth in metals. *Proc. Phys. Soc. Lond.* **60**, 391–394.

O'Hara, K. 1988. Fluid flow and volume loss during mylonitization: an origin for phyllonite in an overthrust setting, North Carolina, U.S.A. *Tectonophysics* **156**, 21–36.

O'Hara, K. 1990. State of strain in mylonites from the western Blue Ridge province, southern Appalachians: the role of volume loss. *J. Struct. Geol.* **12**, 419–430.

Paul, J. B. & Woodward, N. B. 1985. Brittle and ductile evolution of a thrust zone: Thin and thick cataclasites along the Saltville fault. *Geol. Soc. Am. Abs. w. Prog.* **17**, 685–686.

Raj, R. & Chyung, C. K. 1981. Solution–precipitation creep in glass ceramics. *Acta metall.* **29**, 159–166.

Rimstidt, J. D. & Barnes, H. L. 1980. The kinetics of silica–water reactions. *Geochim. cosmochim. Acta* **44**, 1683–1699.

Schmid, S. M. 1975. The Glarus overthrust: Field evidence and mechanical model. *Eclog. geol. Helv.* **68**, 247–280.

Schmid, S. M. 1983. Microfabric studies as indicators of deformation mechanisms and flow laws operative in mountain building. In: *Mountain Building Processes* (edited by Hsu, K. J.). Academic Press, London, 95–110.

Sibson, R. H. 1977. Fault rocks and fault mechanisms. *J. geol. Soc. Lond.* **133**, 191–213.

Simpson, C. 1985. Deformation of granitic rocks across the brittle–ductile transition. *J. Struct Geol.* **7**, 503–511.

Sinha, A. K., Hewitt, D. A. & Rimstidt, J. D. 1986. Fluid interaction and element mobility in the development of ultramylonites. *Geology* **14**, 883–886.

Underwood, E. E. 1970. *Quantitative Stereology*. Addison-Wesley, Reading, Massachusetts.

Van Camp, S. G. & Fullagar, P. D. 1982. Rb–Sr whole-rock ages of mylonites from the Blue Ridge and Brevard zone of North Carolina. *Geol. Soc. Am. Abs. w. Prog.* **14**, 92.

Vernon, R. H. & Flood, R. H. 1988. Contrasting deformation of S- and I-type granitoids in the Lachlan Fold Belt, eastern Australia. *Tectonophysics* **147**, 127–143.

White, S. H. 1976. The effects of strain on the microstructures, fabrics and deformation mechanisms in quartzite. *Phil. Trans. R. Soc.* **A283**, 69–85.

White, S. H. & Knipe, R. J. 1978. Transformation- and reaction-enhanced ductility in rocks. *J. geol. Soc. Lond.* **135**, 513–516.

Wojtal, S. 1986. Deformation within foreland thrust sheets by populations of minor faults. *J. Struct. Geol.* **8**, 341–360.

Wojtal, S. & Mitra, G. 1986. Strain hardening and strain softening in fault zones from foreland thrusts. *Bull geol. Soc. Am.* **97**, 674–687.

Wojtal, S. & Mitra, G., 1988. Nature of deformation in some fault rocks from Appalachian thrusts. In: *Geometry and Mechanisms of Thrusting with Special Reference to the Appalachians* (edited by Mitra, G. & Wojtal, S.). *Spec. geol. Pap. Soc. Am.* **222**, 17–33.

Yonkee, W. A. 1991. Styles and mechanisms of basement deformation within a thrust fault zone, Sevier orogenic belt, northern Utah. *Geol. Soc. Am. Abs. w. Prog.* **23**, A104.